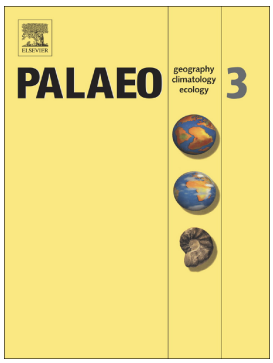

Synchronous onset of the Messinian salinity crisis and diachronous evaporite deposition: New evidences from the deep Eastern Mediterranean basin

Manzi Vinicio, Gennari Rocco, Lugli Stefano, Persico Davide, Roveri Marco, Gavrieli Ittai, Gvirtzman Zohar

PII: S0031-0182(21)00470-3

DOI: https://doi.org/10.1016/j.palaeo.2021.110685

Reference: PALAEO 110685

To appear in: *Palaeogeography, Palaeoclimatology, Palaeoecology*

Received date: 17 June 2021

Revised date: 27 September 2021

Accepted date: 28 September 2021

Please cite this article as: M. Vinicio, G. Rocco, L. Stefano, et al., Synchronous onset of the Messinian salinity crisis and diachronous evaporite deposition: New evidences from the deep Eastern Mediterranean basin, *Palaeogeography, Palaeoclimatology, Palaeoecology* (2021), https://doi.org/10.1016/j.palaeo.2021.110685

Synchronous onset of the Messinian salinity crisis and diachronous evaporite deposition: new evidences from the deep Eastern Mediterranean basin.

Manzi, Vinicio*[1,2], Gennari, Rocco[2,3], Lugli, Stefano[4], Persico Davide[1], Roveri, Marco[1,2], Gavrieli, Ittai[5], Gvirtzman, Zohar [5,6]

* corresponding author

[1] University of Parma, Parma, Italy

[2] ALP, Alpine Laboratory of Palaeomagnetism, Peveragno, CN, Italy

[3] University of Turin, Turin Italy

[4] University of Modena and Reggio Emilia, Modena, Italy

[5] Geological Survey of Israel, Jerusalem, Israel

[6] Hebrew University, Jerusalem, Israel

KEYWORDS

Messinian salinity crisis, onset of evaporites, integrated stratigraphy, Levant basin, Mediterranean

ABSTRACT

We present a basin-wide correlation of the pre-evaporitic succession across the deep Levant basin, based on integrated bio- and cyclostratigraphy. The onset of Messinian

salinity crisis (MSC) can be placed in all studied wells where foraminifers suddenly disappear and normal marine calcareous nannofossils are replaced by opportunistic assemblages. These changes mark the base of the Foraminifers Barren Interval (FBI), a 10s-of-m-thick (below seismic resolution), evaporite-free, shale unit that records the entire duration of the first stage. Moving toward the basin margin the FBI is progressively truncated on top by the Messinian erosional surface (MES), a regional-scale discontinuity sealed by a thin clastic evaporite units overlain by thick halite deposits.

Our results confirm previous hypothesis suggesting that the crisis started in deep- as well as in shallow-water settings at 5.97 Ma and pointing to a synchronous onset of the MSC but diachronous deposition of evaporites. During stage 1 of the crisis, coeval with gypsum deposition in marginal basins, the salinity in deep basins progressively increased (with possible oxygen reduction) hindering the life of marine organisms. Then, at 5.60 Ma, when salinity in deep basins exceeded halite saturation, massive halite precipitation started, and a nearly 2-km-thick salt sequence accumulated in deep basins within a short period of 60 kyr. At that time (stage 2), sedimentation rate jumped by an order of magnitude reaching a few cm/yr. Similar sedimentation rates are inferred for the Realmonte salt mine (Sicily) and observed in the modern Dead Sea and artificial salinas.

1. INTRODUCTION

The Messinian salinity crisis (MSC) is an extreme event in Earth history that occurred ~6 My ago with the widespread accumulation of thick evaporite deposits on the Mediterranean seafloor (Hsü et al., 1973). After half a century of research, the question of a synchronous vs. diachronous onset of the MSC, and particularly the onset and duration of the evaporite deposition in shallow- vs. deep-water Mediterranean settings remains a matter of debate.

The two-step model first proposed by Clauzon et al. (1996) suggested the *synchronous* onset of the crisis in the entire Mediterranean, but the *diachronous* deposition of evaporites, which started in shallow marginal basins (first step) and only later moved to the deeper ones (second step). This scenario was confirmed by studies of intermediate- to deep-water Messinian successions, cropping out in the Apennines, Calabria and Sicily, where stage 1 is represented by evaporite-free deposits (Manzi et al., 2007; Roveri et al., 2008). Working on outcrops allowed the reconstruction of a high-resolution stratigraphic framework through the integration of bio- (foraminifers and calcareous nannofossils), magneto-, cyclo-, and physical-stratigraphic data (Krijgsman et al., 1999; Hilgen and Krijgsman, 1999; Sierro et al., 2001; Krijgsman et al., 2004; Manzi et al., 2007; Dela Pierre at al., 2011; Gennari et al., 2013; Manzi et al., 2013; Roveri et al., 2014a).

These studies led to the establishment of the 3-stage "consensus" model (CIESM, 2008; Roveri et al., 2014a), which accurately defined the onset of the crisis and the deposition of evaporites in shallow- to intermediate-depth settings. But the crisis chronology in the deep-water settings remained a challenge. Data from DSDP (Deep Sea Drillling Project) and ODP (Ocean Drilling Project) cores from the topmost part of the evaporites, have allowed to distinguish between stage 2 and stage 3 deposits and to propose a straightforward correlation with the onshore successions (Roveri et al., 2014b; Lugli et al., 2015). Yet, the lower part of the offshore sections remained unexplored because continuous coring reaching down the pre-evaporitic succession is still lacking. In our opinion, efforts to solve the riddle using only seismic data (e.g., Ochoa et al., 2015; Raad et al., 2020) remain speculative and need to be tested and supported by direct sedimentary observations (see Roveri et al., 2019).

An excellent opportunity to study the deep basin successions has been provided by the drilling campaign for hydrocarbon investigations carried out in the deep Levant Basin in

2009-2012. In fact, this area is presently the only deep basin in the entire Mediterranean from which rock samples from the Messinian evaporites and the underlying Late Miocene succession are available. Albeit these boreholes do not provide continuous coring, rock cuttings and well logs tied to 3D seismic data opened the gate for integrating bio- and cyclostratigraphic studies by two research groups. The two groups reached different conclusions reported in Gvirtzman et al. (2017) and Manzi et al. (2018) on one side, and in Meijlison et al. (2018; 2019) on the opposite one. These studies refueled the old debate concerning the synchronous (Rouchy and Caruso, 2006; Krijgsman et al., 1999) versus diachronous (Butler et al. 1995; Clauzon et al., 1996; Riding et al., 1998; Roveri et al., 2001; 2008) onset of the evaporite deposition (see discussion in Roveri et al., 2014a).

Applying the newly available data and additional tools, Gvirtzman et al. (2017) and Manzi et al. (2018) confirmed the 3-stage model. The model constrained the age of the halite unit from above, by discovering a clastic-rich anhydrite unit (sampled in Or-South-1 borehole), which seals a subaqueous truncation surface (IMTS, intra-Messinian truncation surface) at its top and which, can be assigned to the third stage of the crisis based on its Sr isotope signature. Later, Manzi et al. (2018) performed an integrated stratigraphic study of the pre-evaporitic succession along a deep-shallow transect using three boreholes (Aprhodite-2, Myra-1 and Sara-1) and recognized i) the main key bio-events of the pre-MSC unit (including the *Turborotalita multiloba* distribution), ii) the onset of the MSC at ~5.97 Ma (in Aprhodite-2 and Myra-1) and, iii) an argillaceous evaporite-free unit, barren in foraminifers (FBI) containing an opportunistic calcareous nannofossil assemblage similar to that observed in onshore sections (Manzi et al., 2007; Lozar and Negri, 2019). The recognition of 16 precessional cycles within the FBI in Aphrodite-2 does match the primary selenite gypsum cycles observed in shallow-water settings (PLG, Primary Lower Gypsum, Lugli et al., 2010) suggesting the absence of significant hiatus in the deepest areas where stage 1 is fully recorded by shale; this implies that evaporites deposition began only in

stage 2. Differently, in Myra-1 and Sara-1, which are located closer to the shore, the FBI was found to be partially or completely eroded. In Sara-1 the base of the evaporites is an unconformable surface corresponding to the MES, which progressively cuts deeper towards the continental margin and it is sealed by clastic evaporites derived from the erosion and resedimentation of stage 1 gypsum (Lugli et al., 2013); thus the MES, well-known along the margins, moving in deep settings turns into a conformable surface named MES-cc (Manzi et al., 2018). The integration of the work of Gvirtzman et al. (2017) and Manzi et al. (2018) allow to constrain the timing of halite deposition within stage 2 (~5.60-5.55 Ma), which is consistent with the observations from marginal settings, in agreement with the three stage model (CIESM, 2008; Roveri et al., 2014a,b). The 1700 m-thick salt sequence is sandwiched between the stage 1 shale (FBI) and the stage 3 clastic-rich anhydrite unit (Unit 7 in Gvirtzman et a., 2017), i.e., between the MES-cc and the IMTS. The salt is composed of alternating pure (units 2, 4, 6) and shale-rich layers (units 1, 3, 5), interpreted to record precessional oscillations between relatively arid and relatively humid conditions, (Roveri et al., 2014a; Manzi et al., 2016).

Contrary to the findings described above, the second group analyzed pre-evaporitic samples from Dolphin-1 and did not identify the FBI below the salt dating the base of the evaporites at ~5.89, the mean value between 5.98 and 5.81 Ma (Meijlison et al., 2018, 2019). Based on these findings, Meijlison et al. (2018) challenged the consensus model arguing that salt precipitation in the deep Levant Basin started at around 5.97 Ma, synchronously with the gypsum deposition in the marginal basins. Later, Meijlison et al. (2019), based on seismic reflection counting and well logs analyses carried out in Dolphin-1 and Leviathan-1 boreholes, extended the cyclostratigraphic approach from the pre-evaporitic deposits into the halite unit and dated the 7 seismic units as follows: units 1-4 (stage 1), unit 5 (stage 2) and units 6-7 (stage 3). In summary, Meilijson et. al. (2019) argued that in the deep basin the entire crisis has been recorded by evaporite deposition,

which lasted approximately 640 ky. This implies an evaporite sedimentation rate that is an order of magnitude lower than that postulated by Manzi et al. (2018), who limit the salt deposition to a much shorter period of ~60 ky.

Going beyond the duration and rate of salt accumulation, the controversy between the two opposing views has far-reaching implications concerning the Mediterranean water column during stage 1. Was the deep basin brine at that time saturated (precipitating salt) or diluted (shale accumulation), compared to the sulphate-rich brines in the marginal basins that were precipitating gypsum? A clear answer to this question is essential to implement the hydrological and limnological models for the MSC.

In order to solve this stratigraphic controversy, we have carried out a detailed integrated stratigraphic study on the pre-evaporitic succession sampled in 6 boreholes across the Levant basin (Fig.1): i) Aphrodite-2, Myra-1 and Sara-1, studied by Manzi et al. (2018) are reevaluated here; ii) Dolphin-1, previously studied by Meilijson et al. (2018); and iii) two new boreholes, Tamar-1 and Leviathan-1, whose pre-evaporitic section was still not analyzed (Leviathan-1 is reported in Meijlison et al. 2018 or Meijlison et al., 2019, but not for paleontology). It should be noted that in most wells the sampling resolution is 9 m, but in Aphrodite-2 and Tamar-1 it is 3 m. This difference is highly significant when searching for biostratigraphic datums and key units, such as the FBI, which are only a few tens of meter-thick.

2. METHODS

2.1 Biostratigraphy

The biostratigraphic framework presented here is based on the integration of the data from Manzi et al. (2018) from the Aphrodite-2, Myra-1, and Sara-1 boreholes (38, 23, 12

samples respectively) and the new data from the Leviathan-1, Dolphin-1, and Tamar-1 boreholes (14, 15, 29 respectively).

The sixteen pre-MSC bioevents, referred to in this study are those used for high-resolution tuning of the uppermost pre-evaporitic succession in onshore sections (Hilgen et al., 1999; Sierro et al, 2001; Blanc Valleron et al., 2001; Manzi et al., 2007; Iaccarino et al., 2008; Gennari et al., 2018; Gennari et al., 2020) and are described in the supplementary document (Tab. S1). The table includes also two additional bioevents, that have been defined in onshore sections (Hilgen and Krijgsman, 1999; Sierro et al., 2001), recording influxes of left coiled *Neogloboquadrina acostaensis* with abundance >90% (bioevent x; 6.120 Ma) and >40% (bioevent y; 6.08 Ma) respectively. Since these bioevents are characterized by a very short duration (~10 ky or less), a very high sampling resolution is mandatory for their correct definition. Moreover, these bioevents are sometimes difficult to be identified as right/left ratios have often values close to 50% (Morigi et al., 2007; Gennari et al., 2018). In those case when samples are from cuttings and/or their resolution is low, as for the Levant basin boreholes, the recognition of these bioevents is subjected to errors. Consequently, for our age model we used the distribution of *Turborotalita multiloba* and *N. acostaensis* (both left and right coiled) and, according to Manzi et al. (2018), of the total distribution of foraminifers and calcareous nannofossils. Four bio-intervals were used for wells correlation:

- **TMZ**, *T. multiloba zone* (6.41-5.97 Ma) is the entire fossil distribution zone;
- **TMA**, *T. multiloba* acme (6.21-5.97 Ma) is the fossil distribution zone above its paracme, which includes *N. acostaensis* coiling change occurs at 6.34 Ma;
- **FBI** (Foraminifers barren Interval) is the interval comprised between the highest occurrence (HO) of foraminifers and the base of the evaporites (younger than 5.97 Ma);

- **NBI** (Nannofossils barren interval) is the interval barren in nannofossils found in the upper part of the FBI.

2.2 Cyclostratigraphy

The biostratigraphic timelines described before provided useful anchors to confidently interpret the lithological cycles in the geophysical logs (GR and RES) as precessional cycles, allowing a better tuning of the successions. We applied to Dolphin-1 and Tamar-1 the same methodology of Manzi et al. (2018) for Aphrodite-2, showing that gamma ray (GR) and resistivity (RES) well logs can be successfully utilized to recognize lithological cycles formed by the alternation of light marls and dark-grey shales recorded respectively by “low GR - high RES” and “high GR - low RES” values in the geophysical logs. Using the age of the bioevents in the onshore astronomically-calibrated successions (see Sierro et al., 2001), Manzi et al. (2018) showed that the log-defined lithological cyclicity represents precessional cycles. Accordingly, counting cycles can verify the biostratigraphic age model and can be extrapolated beyond the tie anchors into the FBI.

3. RESULTS

All the boreholes are characterized by consistent foraminifera and nannofossils bioevents, as summarized in the deep-shallow NW-SE transect of Fig.2. Aphrodite-2 and Tamar-1 boreholes are particularly significant for the higher sampling resolution, which allows a better identification of bioevents. The count of lithological cycles defined from the geophysical logs (gamma ray and resistivity) has been utilized to check the consistency of the bioevents distribution in the different boreholes and their correlation. The thickness of the sampled interval (th) and the sampling interval (si) are reported below for each borehole.

*Aphrodite-2 (th: **3** m; si: **3** m)* - this borehole represents the deepest Messinian portion of the Levant basin. The data confirm the results of Manzi et al. (2018). Bioevents 5, 6, 7, 8, 10, 11 and 14 allow the precise definition of the crisis onset and the recognition of the TMA and FBI with thicknesses of 40 m and 27 m, respectively. The latter, based on the recognition of 16 GR-defined lithological cycles, completely records the time interval of stage 1 (Manzi et al., 2018). In this interval, and similarly to what observed onshore (Manzi et al., 2007), the nannofossils are represented by opportunistic species (including *Sphenolithus abies*, *Helicosphaera carteri*, *Reticulofenestra minuta*, *Reticulofenestra antarctica* and *Umbilicosphaera rotula*; see Manzi et al., 2018) in the lower part of the FBI and completely disappear upwards, allowing the recognition of the NBI.

*Leviathan-1 (th: **9** m; si: **9** m)* - in this borehole the definition of the bioevents is more complicated due to the higher terrigenous content and greater reworking; nonetheless, the TMZ and TMA have been defined with good precision allowing to recognize the possible position of bioevent 5. The interval containing *T. multiloba* is thicker (~70 m) than in Aphrodite-2, probably due to the higher sedimentation rate. Conversely, the FBI is thinner, around 10-m thick; the recognition of only 5 GR-defined lithological cycles suggest that the FBI is eroded at its top.

*Dolphin-1 (th: **3** m; si: **9** m)* - The distribution of *T. multiloba* has been defined with good precision and in good agreement with the distribution zone of right coiled *N. acostaensis*. The thicknesses of the TMZ and TMA are respectively ~50 m and ~32 m, like in Aphrodite-2. The FBI is ~25 m-thick and consists of 13-14 GR-defined lithological cycles. The NBI has been identified in its upper portion, similarly to Aphrodite-2. These results differ from those of Meilijson et al. (2018), who did not identify neither the *T. multiloba* distribution nor the FBI in Dolphin-1.

*Tamar-1 (th: **3** m; si: **3** m)* - in this borehole the best biostratigraphic tie-point are the *N. acostaensis* L/R coiling change and the distribution of *T. multiloba*. Here the TMZ shows a thickness of ~35 m. The FBI is ~20 m-thick with 11 GR-defined lithological cycles. The NBI is located in the upper portion of the FBI, similarly to Aphrodite-2 and Dolphin-1.

*Myra-1 (th: **3** m; si: **9** m)* - here the occurrence of the foraminifers is more discontinuous with respect to the other boreholes and recognition of bioevents is less straightforward. However, the distribution of *T. multiloba* and *N. acostaensis* allow to tentatively define the *N. acostaensis* L/R coiling change ~20 m below the highest occurrence (HO) of foraminifera, similarly to Tamar-1. The FBI is ~23 m-thick and the NBI is located in its upper part.

*Sara-1 (th: **3** m; si: **3** m)* - based on the distribution of *T. multiloba* and *N. acostaensis,* the *N. acostaensis* L/R coiling change can be placed very close to the base of the evaporites. The FBI is not present. These data suggest the existence of a large stratigraphic hiatus in association with the MES at the base of the evaporites.

4. THE SINCRHONOUS ONSET OF THE MSC AND THE DIACHRONOUS DEPOSITION OF THE EVAPORITES

4.1 The onset of the Messinian salinity crisis in the deep Levant basin

The results of the biostratigraphic analyses provide a robust basin-wide correlation panel from the deepest (Aphrodite-2) to the shallowest (Sara-1) part of the basin (Fig. 2) based on the combined distribution range of *T. multiloba* and *N. acostaensis*, (both left and right coiled), integrated with the distribution of the calcareous nannofossils.

The pre-MSC succession is continuous and quite homogeneous across the basin; the recognition of the TMA and TMZ biozones in all the boreholes confirms their reliability and usefulness in offshore boreholes, as already demonstrated for onshore successions.

Differently, the thickness of the FBI, the number of lithological cycles within it and the thickness (or complete absence) of the NBI change laterally across the basin, as previously observed both in shallow- (Manzi et al., 2007) and in deep-water settings (Manzi et al., 2018). In the depocentral area (Aphrodite-2) up to 16 cycles recording the whole duration of stage 1 have been recognized in the FBI. In the other boreholes the reduced number of cycles suggests that the FBI has been truncated on top, at the base of the evaporites. The conformable base of the FBI and its unconformable top indicate post-depositional truncation by the MES. The amount of erosion associated to the base of unit 0 is minimal or nearly zero (MES-cc) in the deeper settings (Aphrodite-2) and progressively increases landward up to ~700 ka in the Sara-1 borehole, where the entire FBI and part of the underlying pre-MSC lower Messinian interval (TMZ zone) are eroded. Flattening all the boreholes to the FBI base datum highlights the synchronous onset of the MSC as a conformable boundary. This stands in contrast to the transition from stage 1 to stage 2 (Manzi et al., 2018 and this work) and the transition from stage 2 to stage 3 (Gvirtzman et al., 2017), which represent erosional unconformities.

Our age model is different to that of Meilijson et al. (2018), which is based only on bioevents of the *N. acostaensis* (the L/R coiling change and the two influxes of sinistral coiled specimens; bioevents 5, x and y in tab. 1) as they did not used or identified the distribution of *T. multiloba.*

Following the experience gained in the uppermost pre-MSC onshore successions (Hilgen et al., 1999; Sierro et al, 2001; Blanc Valleron et al., 2001; Manzi et al., 2007; Iaccarino et al., 2008; Gennari et al., 2018; Gennari et al., 2020) we note that *T. multiloba* is always

present and represents a very valuable tool for the biostratigraphy of the uppermost pre-MSC interval. In contrast the influxes of sinistral specimens used by Meilijson et al. (2018) are difficult to pick, even in onshore successions, due to their very short duration (~10 ky or less); thus, their reliability is reduced when sampling resolution is low. Moreover, above the TMZ, the FBI in Dolphin-1 is represented by only two samples (one with reworked foraminifers) separated by a 9 m interval. Probably for this reason, Meilijson et al. (2018) did not consider the possible presence of the FBI. Conversely, in Aphrodite-2 and in Tamar-1 the FBI has been recognized with a higher number of samples (nine and six respectively) devoid of foraminifers (Fig. 2).

Thus, based on the presence of the FBI in 5 boreholes, the NBI in 4 wells, and the recognition of bioevents 4, 6, 7, 9, 10, 11, and 14 (Table 1, supplementary material), we suggest that the presence of the stage 1 evaporite-free interval is robust. Consequently, we raise the possibility that the upper pre-MSC portion of the age model of Meijlison et al., (2018) could be erroneous.

A consequence of the possible erroneous age model reconstructed by Melijison et al. (2018) in Dolphin-1 is the anomalously high sedimentation rate of ~15.9 cm/ka (Fig. DR1, supplementary material) between their bioevent 5 (influx of sinistral neogloboquadrinids; 6.127 Ma) and the base of the evaporites, placed at 5.97 Ma. This anomaly does not appear in our interpretation of Dolphin-1 that allow to assign an age of ~ 5.70 Ma to the topmost pre-evaporite sample on the basis of a) the extrapolation of the sedimentation rate between bioevents 10 and 6 and b) the number of cycles in the FBI.

Our interpretation of the pre-evaporitic succession in Dolphin-1 is further supported by comparing the sedimentation rate to that of Aphrodite-2 (Manzi et al., 2018) and Tamar-1 (this study), where the sampling resolution is three times higher. According to our chronology, all three wells exhibit quite homogeneous sedimentation rates of around 9

cm/ka (Fig. 3). The recognition of a reduced, probably incomplete, FBI in Dolphin-1, compared with that found in Aphrodite-2, points for an upper truncation of the FBI that is confirmed by seismic. The thinning of the FBI due to the truncation is below seismic resolution, but a hint for the thinning of the combined FBI+TMZ (>50 m thick) can be identified in a seismic profile crossing Dolphin-1 (Fig 4c and Fig. DR2 taken from Fig. DR1 of Meilijson et al., 2018), where the yellow reflector (YR), which roughly coincides with the base of the TMZ (see Fig. 2), and the light blue one (BR), corresponding to the base of the evaporites (unit 0; made up of anhydrite), converge southeastwards. The thinning of the YR-BR interval (Fig. 4c and DR2) is consistent with the regional truncation shown in Fig. 2 indicating an unconformable character for the base of the evaporites, which can be regarded as the MES.

4.2 The onset and duration of evaporites deposition in the deep Levant basin

The revised age model of the pre-salt succession directly affects the cyclostratigraphic interpretation of the overlying salt sequence. We suggest that overlooking the FBI (duration of 370 ky) below the evaporites, Meilijson et al. (2018, 2019) wrongly concluded that the evaporitic sequence of the Levant basin starts at 5.97 Ma and represents the entire MSC (640 ky). Meilijson et al. (2018, 2019) also assumed that the well logs and seismic reflections in the evaporite sequence can be used for cycle counting. Accordingly, they interpreted their 32 “seismic cycles”, as representing precession cycles (640/32=20 ky). However, in our opinion this cyclostratigraphic interpretation is based on an erroneous age model, as the authors did not explain in terms of lithological cyclicity and climatic variations the nature of the single precessional cycle imaged by seismic. In our view, the cyclostratigraphic use of well logs (GR and RE) and seismic reflections, is not straightforward because: i) the quality of the resistivity logs in evaporites and the significance of the observed fluctuations is questionable; ii) the number of seismic

reflections depends on the vertical seismic resolution, which in turn depends on a number of variables characterizing the rock properties (seismic velocity, depth), as well as seismic acquisition and processing parameters (dominant frequency); see discussion in Roveri et al. (2019); iii) the correspondence between the cycles defined in the geophysical logs and in the seismic sections is not clear; iv) the authors admit that the cyclicity in the lower part of the Main Halite interval (cycles 1-11) is not easily recognized; v) the seismic profiles are characterized by a strong lateral variability in the total number of reflectors that cast some doubts about their cyclostratigraphic significance (Meilijson et al. 2019; see lateral variations within 0.5 to 1 km aside wells Dolphin-1 and Leviatnan-1 in their figure 5); vi) the authors did not explain in terms of lithological cyclicity and climatic variations the nature of a single precessional cycle imaged by seismic and; vii) the authors completely overlooked the smaller-scale cyclicity that can be recognized from the geophysical logs.

The cyclostratigraphic interpretation of the salt sequence presented in this work is anchored by absolute ages at its base and top. The base is the onset of stage 2 (5.6 Ma, Manzi et al., 2018 and this work), which is marked by the Messinian erosional surface (MES) in most of the boreholes and by its correlative conformity (MES-cc) in Aphrodite-2 (no hiatus). The accumulation of halite was preceded by the deposition of a thin clastic evaporites unit that can be followed upslope in the canyons excavated in the Israeli continental margin (Fig. 1; Lugli et al., 2013). The top of the halite is the onset of stage 3, which is marked by the intra-Messinian truncation surface (IMTS; Gvirtzman et al. 2017). This surface separates two very different units, expressing different depositional and hydrological settings. The lower unit, truncated at its top by the IMTS, mainly consist of km-thick massive halite deposits, which show geochemical affinity with the evaporites of stage 1 and 2 found onshore. Conversely, the unit laying above the truncation surface is composed of terrigenous deposits with only minor evaporitic component and Lago Mare fauna; the evaporites of the upper unit are largely sulphates and are characterized by a

very distinct geochemical signature compared to that of the lower units. For these reasons Gvirtzman et al. (2017) linked the development of the IMTS to the moment when halite precipitation was interrupted by the arrival of hypohaline waters in the Mediterranean, which also dissolved the upper part of the halite sequence at shallower depth. They proposed an age of 5.54 Ma for the formation of the IMTS, but small age refinements cannot be excluded. The direct implication of these age anchors is that the ~1700 m-thick salt sequence in the deep basin, which includes ~3 precessional cycles (Fig. 4), records only ~60 ka (stage 2) instead of 640 ka (Meilijson et al., 2019). This further implies that the thickness of the precessional cycles in the salt sequence are in the order of hundreds of meters. Following Manzi et al. (2016; 2018), we suggest that these cycles are expressed by alternations of pure salt units (transparent seismic facies, units 2, 4, 6) and clastic-rich salt units (stratified facies, units 1, 3, 5, 7 with higher terrigenous component). Such lithological cycles could record the oscillations between relatively arid and humid conditions (Manzi et al., 2016, 2018). Our interpretation also implies a yearly accumulation of a few cm-thick halite varves (~1.7 cm, accumulated in ~60 ka), which are below well-log resolution. As for the smaller scale cycles, dm- to m-thick, observed in the geophysical logs by Meilijson et al. (2019), we argue that they could represent sets of pluriannual halovarves, possibly dominated by ~10 years lunar-solar cycles. Such cycles are best observed in the Realmonte salt mine in Sicily (Manzi et al., 2012), where the most continuous record of primary annual cycles can be observed. We also note that our calculated sedimentation rate for halite is consistent with those observed in the Realmonte section, in the present-day Dead Sea, and in artificial salinas, whereas according to Meilijson (2019) the halite accumulation rate in the deep basin was very low, similar to that observed for primary gypsum deposited at the shallower depths in stage 1 (PLG) and 3 (UG) (Fig. 5).

Settling the stratigraphic debate discussed above has far reaching implications on the development of the marine conditions in the MSC. According to Meilijson's model, in the first stage of the crisis salt precipitated in the deep basin (Units 1-4); in the second stage, when sea-level dropped, huge amount of eroded gypsum arrived in the deep basin and formed a 200-400 m thick clastic anhydrite layer (seismic unit 5); in stage 3.1 salt precipitation resumed (Meilijson et al., 2019). Nevertheless, this scenario is not confirmed by data. In fact, well log analyses and cuttings samples (Gvirtzman et al., 2017; Aprodite-2) indicate that seismic unit 5 is mostly composed of halite, not anhydrite. The redeposited particles described by Meilijson et al., (2019) are present in the shale interbeds, but the greatest part is actually salt, as indicated by log interpretation (Feng et al., 2016; Gvirtzman et al., 2017). Moreover, it is difficult to reconcile the interruption of halite precipitation in the deep basin during the acme of the crisis in stage 2, while massive amount of salt was deposited in the intermediate basins (Roveri et al., 2014a).

4.3 Paleoceanographic Implications for the MSC

The presence of an evaporite-free succession representing the deep-water counterpart of the bottom-grown Primary Lower Gypsum deposits developed in marginal shallow settings has important implications for the reconstruction of the hydrology of the Mediterranean during stage 1. The absence of evaporites suggest undersaturation with respect to gypsum in the deep setting due to the presence of a gypsum compensation depth surface marking the upper limit of a deep anoxic zone where physical, geochemical and biological characteristics prevented accumulation and/or precipitation (De Lange and Krijgsman, 2010; Dela Pierre et al., 2011; Roveri et al., 2014a; Roveri et al., 2020). Indeed, a similar setting was observed in the Dead Sea in the 1950s' when gypsum accumulated on the seafloor down to the depth of the epilimnion, whereas nearly no

gypsum was found on the seafloor of the anoxic, H_2S-rich hypolimnion (Neev and Emery, 1967).

An important role in conditioning the distribution of the brine from which the PLG precipitated could have also been played by the presence of morpho-structural sills. which may have favored the formation of the brine in semi-isolated basins (Roveri et al., 2014a). This still open question in the Messinian salinity crisis is well beyond the aim of our paper and need to be addressed to future works.

5. SUMMARY AND CONCLUSIONS

The results of our integrated stratigraphy study in the deep Levant Basin can now be summarized as follows:

- The MSC onset in deep basin is marked by the sudden disappearance of foraminifers and by a sharp change of calcareous nannofossils from normal marine to opportunistic assemblages, similarly to changes observed onshore (Manzi et al., 2007; Lozar and Negri, 2019).
- Stage 1 in the deep Levant basin is fully recorded by an organic-rich evaporite-free shale unit, which is barren in foraminifers (FBI); the disappearance of the nannofossils, in the upper part of the FBI marks the base of the NBI. The FBI is characterized by a sedimentation rate of ~9 cm/ky, similar to that of the pre-MSC sequence.
- The transition from stage 1 to stage 2 is marked by a conformable boundary in the deepest part of the basin (MES-cc) that becomes erosive (MES) and progressively truncates stage 1 and even older deposits towards the coast.

- Stage 2 began with the deposition of a few meter-thick gypsum layer, which quickly changed to rapid salt deposition to form a 1700 m-thick sequence. The thin gypsum layer below the salt correlates with the clastic evaporites of the resedimented lower gypsum found upslope in the canyons of the Israeli margin (Lugli et al., 2013). The rate of salt deposition was three orders of magnitudes higher than that of the shales below, reaching a few cm/y, similar to that observed in the Realmonte salt mine (Sicily) and comparable to the halite precipitation rates in the modern Dead Sea and artificial salinas.
- Our results suggest that during stage 1 the Mediterranean water column was characterized by a progressive rise in salinity (and possible oxygen reduction), which increasingly hindered the life of the marine organism, and that primary gypsum deposition was limited to shallow-water marginal basins. Such a rise in salinity can be considered a preconditioning phase during which the water column was approaching halite saturation. The latter was attained only during stage 2, when massive halite precipitation and accumulation took place.
- During stage 1, no evaporites, neither sulphates nor halite, precipitated in the deep settings; this observation is in odds with studies based only on geophysical data (Ochoa et al., 2015; Raad et al., 2020) as well as with Meijlison et al., 2019, who based their biostratigraphic analysis on a single well (Dolphin-1), where the FBI can easily be missed. Our results, call for great prudence while inferring the true nature and stratigraphic position of evaporite sediments without a direct analysis of the sediment themselves (see discussion in Roveri et al., 2019).

All these findings confirm the scenario originally proposed by Clauzon et al. (1996) and later modified by CIESM (2008) and Roveri et al. (2014a), which envisages a synchronous onset of the crisis in deep as well as in shallow-water settings at 5.97 Ma

and a diachronous evaporite deposition by the precipitation of gypsum in shallow settings during stage 1 and halite in the deep basins during stage 2 (after 5.60 Ma).

ACKNOWLEDGMENTS

We acknowledge Modi'in Energy and Pelagic partnership for their permission to release data related to the wells Aprodite-2, Myra-1, and Sara-1. Delek Drilling are acknowledged for the permission to use seismic data and well data for Leviathan-1, Tamar-1, and Dolphin-1. We thank HIS Markit for providing us the Kingdom academic licenses for seismic interpretation. This work has benefited from the equipment and framework of the COMP-HUB Initiative, funded by the 'Departments of Excellence' program of the Italian Ministry for Education, University and Research (MIUR, 2018-2022). Amorosi A. and Aloisi G. are greatly acknowledged for their suggestions aimed to improve an earlier version of the manuscript.

REFERENCES

Bertoni, C., Cartwright, J., 2007a. Major erosion at the end of the Messinian Salinity Crisis: evidence from the Levant Basin, Eastern Mediterranean. Basin Research 19, 1–18.

Blanc-Valleron, M.M., Pierre, C., Caulet, J.P., Caruso, A., Rouchy, J.M., Cespuglio, G., Sprovieri, R., Pestrea, S., Di Stefano, E., 2002. Sedimentary, stable isotope and micropaleontological records of paleoceanographic change in the Messinian Tripoli Formation (Sicily, Italy). Palaeogeography, Palaeoclimatology, Palaeoecology 185, 255–286.

Buchbinder, B., And Zilberman, E., 1997, Sequence stratigraphy of Miocene–Pliocene carbonate–siliciclastic shelf deposits in the eastern Mediterranean margin (Israel): effects of eustasy and tectonics: Sedimentary Geology, v. 112, p. 7–32.

Butler, R.W.H., Likhorish, W.H., Grasso, M., Pedley, H.M., Ramberti, L., 1995. Tectonics and sequence stratigraphy inMessinian Basins, Sicily: constraints o the initiation and termination of the Mediterranean salinity crisis. Geological Society of America Bulletin 107, 425–439.

CIESM, 2008. The Messinian salinity crisis from mega-deposits to microbiology. In: Briand, F. (Ed.), A consensus report, in 33ème CIESM Workshop Monographs, 33. CIESM, 16, bd de Suisse, MC-98000, Monaco, pp. 1–168.

Clauzon, G., Suc, J.-P., Gautier, F., Berger, A., Loutre, M.F., 1996. Alternate interpretation of the Messinian salinity crisis, controversy resolved? Geology 24, 363–366.

Cohen, A., 1993, Halite–clay interplay in the Israeli Messinian: Sedimentary Geology, v. 86, p. 211–228.

De Lange, G.J., Krijgsman, W., 2010. Messinian salinity crisis: a novel unifying shallow gypsum/deep dolomite formation mechanism. Marine Geology 275, 273-277.

Dela Pierre, F., Bernardi, E., Cavagna, S., Clari, P., Gennari, R., Irace, A., Lozar, F., Lugli, S., Manzi, V., Natalicchio, M., Roveri, M., Violanti, D., 2011. The record of the Messinian salinity crisis in the Tertiary Piedmont Basin (NW Italy): the Alba section revisited. Palaeogeography, Palaeoclimatology, Palaeoecology 310, 238–255.

Feng, Y. E., Ynkelzon, A., Steingberg, J., & Reshef, M., 2016. Lithology and characteristics of the Messinian evaporite sequence of the deep Levant Basin, eastern Mediterranean. Marine Geology, 376, 118–131.

Gennari, R., Manzi, V., Angeletti, L., Bertini, A., Biffi, U., Ceregato, A., Taviani, M., 2013. A shallow water record of the onset of theMessinian salinity crisis in the Adriatic foredeep (Legnagnone section, Northern Apennines). Palaeogeography, Palaeoclimatology, Palaeoecology, 386, 145–164.

Gennari, R., Lozar, F., Turco, E., Dela, Pierre F., Lugli, S., Manzi, V., Taviani, M., 2018. Integrated stratigraphy and paleoceanographic evolution of the pre-evaporitic phase of the Messinian salinity crisis in the Eastern Mediterranean as recorded in the Tokhni section (Cyprus Island). Newsletters on Stratigraphy, 51(1), 33–55.

Gennari, R., Lozar, F., Natalicchio, M., Zanella E., Carnevale, G., Dela Pierre, F., 2020. Chronology of the Messinian events in the northern ost part of the Mediterranean: the Govone section (Piedmont basin, NW Italy). Rivista Italiana di Paleontologia e Stratigrafia (Research in Paleontology and Stratigraphy), vol. 126(2): 541-560. July 2020

Gvirtzman, Z., Manzi, V., Calvo, R., Cavireli, I., Gennari, R., Lugli, S., Roveri, M., 2017. Intra-Messinian truncation surface in the Levant Basin explained by subaqueous dissolution. Geology, 45, 915–918.

Hilgen, F. J., & Krijgsman, W., 1999. Cyclostratigraphy and astrochronology of the Tripoli diatomite formation (pre-evaporite Messinian, Sicily, Italy). Terra Nova, 11, 16–22.

Hsü, K., Ryan,W.B.F., Cita, M., 1973. Late Miocene desiccation of the Mediterranean. Nature, 242, 240.

Iaccarino, S.M., Bertini, A., Di Stefano, A., Ferraro, L., Gennari, R., Grossi, F., Lirer, F., Manzi, V., Menichetti, E., Ricci Lucchi, M., Taviani, M., Sturiale, G., Angeletti, L., 2008. The Trave section (Monte dei Corvi, Ancona, Central Italy): an integrated paleontological study of the Messinian deposits. Stratigraphy 5, 281–306.

Krijgsman,W., Hilgen, F.J., Raffi, I., Sierro, F.J., Wilson, D.S., 1999b. Chronology, causes, and progression of the Messinian salinity crisis. Nature 400, 652–655.

Krijgsman, W., Gaboardi, S., Hilgen, F.J., Iaccarino, S., de Kaenel, E., van der Laan, E., 2004. Revised astrochronology for the Ain el Beida section (Atlantic Morocco): no glacioeustatic control for the onset of the Messinian Salinity Crisis. Stratigraphy 1, 87–101.

Lozar, F., Negri, A., 2019. A review of basin-wide calcareous nannofossil bioevents in the Mediterranean at the onset of the Messinian salinity crisis. Marine Micropaleontology, 151: 101752.

Lugli, S., Manzi, V., Roveri, M., Schreiber, B.C., 2010. The Primary Lower Gypsum in the Mediterranean: a newfacies interpretation for the first stage of theMessinian salinity crisis. Palaeogeography, Palaeoclimatology, Palaeoecology 297, 83–99.

Lugli, S., Gennari, R., Gvirtzman, Z., Manzi, V., Roveri, M., Schreiber, B.C., 2013. Evidence of clastic evaporites in the canyons of the Levant Basin (Israel): implications for the Messinian Salinity Crisis. Journal of Sedimentary Research 83, 942–954

Lugli, S., Manzi, V., Roveri, M., & Schreiber, C., 2015. The deep record of the Messinian salinity crisis: Evidence of a non-desiccated Mediterranean Sea. Palaeogeography, Palaeoclimatology, Palaeoecology, 433, 201–218. ttps://doi.org/10.1016/j.palaeo.2015.05.017

Manzi, V., Roveri, M., Gennari, R., Bertini, A., Biffi, U., Giunta, S., Iaccarino, S.M., Lanci, L., Lugli, S., Negri, A., Riva, A., Rossi, M.E., Taviani, M., 2007. The deep-water counterpart of the Messinian Lower Evaporites in the Apennine foredeep: the Fanantello section (Northern Apennines, Italy). Palaeogeography, Palaeoclimatology, Palaeoecology 251,470–499.

Manzi, V., Gennari, R., Lugli, S., Roveri, M., Scafetta, N., Schreiber, B.C., 2012. High frequency cyclicity in the Mediterranean Messinian evaporites: evidence for solar–lunar climate forcing. Journal of Sedimentary Research 82, 991–1005.

Manzi, V., Gennari, R., Hilgen, F., Krijgsman, W., Lugli, S., Roveri, M., Sierro, F.J., 2013. Age refinement of theMessinian salinity crisis onset in theMediterranean. Terra Nova 25, 315–322.

Manzi, V., Lugli, S., Roveri, M., Dela, Pierre F., Gennari, R., Lozar, F., Turco, E., 2016. The Messinian salinity crisis in Cyprus: A further step towards a new stratigraphic framework for Eastern Mediterranean. Basin Research, 28, 207–236.

Manzi, V., Gennari, R., Lugli, S., Persico, D., Reghizzi, M., Roveri, M., Gvirtzman, Z., 2018. The onset of the Messinian salinity crisis in the deep Eastern Mediterranean Basin. Terra Nova, 30, 189–198. doi:10.1111/ter.1232530, 189-198

Meilijson, A., Steinberg, J., Hilgen, F., Bialik, O. M., Waldmann, N. D., & Makovsky, Y., 2018. Deep-basin evidence resolves a 50-year-old debate and demonstrates synchronous onset of Messinian evaporites in a non-desiccated Mediterranean. Geology, 46, 243–246.

Meilijson, A., Hilgen, F., Sepúlveda, J., Steinberg, J., Fairbank, V., Flecker, R., Waldmann, N.D., Spaulding, S.A., Bialik, O.M., Boudinot, F.G., 2019. Chronology with a pinch of salt: integrated stratigraphy of Messinian evaporites in the deep East-ern Mediterranean reveals long-lasting halite deposition during Atlantic connectivity. Earth Sci. Rev. 194, 374–398.

Morigi, C., Negri, A., Giunta, S., Kouwenhoven, T., Krijgsman, W., Blanc-Valleron, M.M., Orszag-Sperber, F., Rouchy, J.M., 2007. Integrated quantitative biostratigraphy of the

latest Tortonian-early Messinian Pissouri section (Cyprus): An evaluation of calcareous plankton bioevents. Geobios, 40: 267-279.

Neev, D., Emery, K.O., 1967. The Dead Sea: Depositional Processes and Environments of Evaporites. Israel Geological Survey Bulletin 41, 147 p.

Ochoa, D., Sierro, F. J., Lofi, J., Maillard, A., Flores, J.-A., & Suarez, M., 2015. Synchronous onset of the Messinian evaporite precipitation: First Mediterranean offshore evidence. Earth and Planetary Science Letters, 427, 112–124. doi:10.1016/j.epsl.2015.06.059

Raad, F., Lofi, J., Maillard, A., Tzevahirtzian, A., Caruso, A., 2020. The Messinian Salinity Crisis deposits in the Balearic Promontory: An undeformed analog of the MSC Sicilian basins? Marine and Petroleum Geology, 121, 104777

Riding, R., Braga, J.C., Martín, J.M., 1999. Late Miocene Mediterranean desiccation: topography and significance of the 'Salinity Crisis' erosion surface on-land in southeast Spain. Sedimentary Geology 123, 1–7.

Rouchy, J.M., Caruso, A., 2006. TheMessinian salinity crisis in theMediterranean basin: a reassessment of the data and an integrated scenario. Sedimentary Geology 188, 35–67.

Roveri, M., Bassetti, M.A., Ricci Lucchi, F., 2001. TheMediterranean Messinian Salinity Crisis: an Apennine foredeep perspective. Sedimentary Geology 140, 201–214.

Roveri, M., Lugli, S., Manzi, V., Schreiber, B.C., 2008b. The Messinian Sicilian stratigraphy revisited: toward a new scenario for the Messinian salinity crisis. Terra Nova 20, 483–488.

Roveri, M., Flecker, R., Krijgsman, W., Lofi, J., Lugli, S., Manzi, V., Sierro, F.J., Bertini, A., Camerlenghi, A., De Lange, G., Govers, R., Hilgen, F.J., Hübscher, C., Meijer, P.Th,

Stoica, M., 2014a. The Messinian Salinity Crisis: Past and future of a great challenge for marine sciences. Marine Geology, 352, 25–58.

Roveri, M., Lugli, S., Manzi, V., Gennari, R., Schreiber, B. C., 2014b. High-resolution strontium isotope stratigraphy of the Messinian deep Mediterranean basins: Implications for marginal to central basins correlation. Marine Geology, 349, 113–125.

Roveri, M., Gennari, R., Ligi, M., Lugli, S., Manzi, V., Reghizzi, M., 2019. The synthetic seismic expression of the Messinian salinity crisis from offshore records: implications for shallow- to deep-water correlations. Basin Res. 31, 1121–1152.

Roveri, M., Lugli, M., Manzi, V., Reghizzi, M., Rossi, F.P., 2020. Stratigraphic relationships between shallow-water carbonates and primary gypsum: insights from the Messinian succession of the Sorbas Basin (Betic Cordillera, Southern Spain), Sedimentary Geology, 404, 105678, doi:10.1016/j.sedgeo.2020.105678.

Laskar, J., Fienga, A., Gastineau, M., & Manche, H., 2011. La2010: A new orbital solution for the long-term motion of the Earth. Astronomy & Astrophysics, 532, A89.

Sierro, F. J., Hilgen, F. J., Krijgsman, W., Flores, J. A., 2001. The Abad composite (SE Spain): A Messinian reference section for the Mediterranean and the APTS. Palaeogeography, Palaeoclimatology, Palaeoecology, 168, 141–169.

FIGURE CAPTIONS

Fig. 1 - Location map of the Levant basin with the distribution of thin and thick Evaporitic Units (EU) (modified after Manzi et al., 2016) together with the evaporitic seismic onlap (ESO, from Bertoni and Cartwright, 2007) and the evaporite up dip limit (EUL, from Buchbinder and Zilberman 1997 and Cohen 1993). Offshore boreholes penetrating the thick evaporite sequence and reaching the pre-evaporitic succession are marked by yellow

circles. Onshore boreholes crossing a thinner evaporite section and studied by Lugli et al. (2013) are marked by orange circles. The trace of the Ashdod and Afiq canyons is marked by blue arrows. ISR- Israel; JOR – Jordan; EGY – Egypt; LBY - Lybia.

Fig. 2 - Deep-shallow NW-SE correlation panel of the studied boreholes reporting the biostratigraphic events and the geophysical logs (GR, gamma ray in green; RES, resistivity in red). The onset of the MSC is used as datum plain. Blue-squared numbers are the bio-magneto stratigraphic events (see Tab. S1 for full references): 1) HO *G. nicolae* (6.710 Ma); 2) LO *N. amplificus* (6.684 Ma); 3) HO *G. miotumida* (6.500 Ma); 4) LO *T. multiloba* (6.410 Ma); 5) L/R *N. acostaensis* coiling change (6.340 Ma) = MMi3c base; 6) AB *T. multiloba* (6.210 Ma); 7) AE *T. multiloba* (6.040 Ma); 8) base of Gilbert chron (6.035 Ma); 9) AP of S. abies (5.974 Ma); 10) HO foraminifera (5.971 Ma) = base of Non-Distinctive Zone; 11) HCO normal marine calcareous nannofossils (5.970 Ma); 12) sharp decrease in abundance and diversity of calcareous nannofossils (5.970 Ma); 13) HO *N. amplificus* (5.939 Ma); 14) HO calcareous nannofossils (5.750-5.640 Ma); 15) HO *D. quinqueramus* (5.540 Ma). Black-squared numbers indicate the inferred age of uppermost pre-evaporitic deposits in Ma. Black arrows indicate samples positions. SI, 65°N summer insolation; E, Eccentricity (Laskar 2004).

Fig. 3 - Estimated sedimentation rates for the Dolphin-1, Aphrodite-2 and Tamar-1 boreholes.

Fig. 4 - (A) Astronomical tuning of the seismic units in the Levant Basin MSC sequence. Note that while stage 1 (370 kyr; 16 precessional cycles) is represented by a 10s-of-m-thick shale unit (below seismic resolution) and stage 3 (220 kyr; 10 cycles) is represented by ~100 m thick clastic-rich anhydrite unit, the much shorter stage 2 (60 kyr; 3 cycles) is represented by an extremely thick (1700 m) salt sequence. Closer view of the unconformities above (IMTS, inset B) and below (MES, inset C) the salt near the Dolphin-1

borehole. Note that the truncation of the FBI+TMZ interval by the MES is recognized by seismic.

Fig. 5 - Mean sedimentation rates for the Messinian units: shales of the pre-MSC (gray), of the pre-MSC+FBI (blu), of the FBI only (black); gypsum/shale and gypsum only of the PLG (purple) and of the UG (fucsia) units; halite of Messinian (green) and modern Dead Sea and salina (white). Full refefences available in table 1 (DR). Notice that the sedimentation rate of the salt unit in the Levant basin is smaller than the sedimentation date of the stage 1 primary gypsum (PLG unit, Lugli et al., 2010)

Declaration of interests

☒ The authors declare that they have no known competing financial interests or personal relationships that could have appeared to influence the work reported in this paper.

☐The authors declare the following financial interests/personal relationships which may be considered as potential competing interests:

The Authors:

Vinicio Manzi, Rocco Gennari, Stefano Lugli, Davide Persico, Marco Roveri, Ittai Gavrieli, Zohar Gvirtzman.

Highlights

- The onset of the Messinian salinity crisis was synchronous at 5.97 Ma
- In the deep Levant basin the onset is marked by the disappearance of marine biota
- Evaporite-free shales barren in foraminifers record stage 1 of the crisis
- The evaporite succession started to accumulate in deep settings only since stage 2
- A regional-scale unconformity marks the base of the evaporites